

Kinetic Study of Methyl Orange Adsorption on Activated Carbon Derived from Pine (*Pinus strobus*) Sawdust

Sobhy M. Yakout,^{a,*} Mohamed R. Hassan,^b Mohamed E. El-Zaidy,^c and Omar H. Shair,^c and Abdalrhaman M. Salih^c

Pine (*Pinus strobus*) sawdust (PSD), a sawmill waste, was used as a precursor for the preparation of activated carbon through a chemical activation technique with phosphoric acid at 600 °C (100 min). Phosphoric acid pine sawdust activated carbon (PSDP) was characterized and used for the adsorption of methyl orange (MO). The textural examination was applied to determine the total pore volume and specific surface area of PSDP. Carbon surface functional groups were identified utilizing Fourier transform infrared spectroscopy. The effects of pH, contact time, and adsorbent mass on the sorption were investigated in a batch procedure mode. Kinetic information was studied that followed the pseudo-second-order model. The results showed that PSDP could be used as a low-cost adsorbent for MO adsorption from waste effluents.

Keywords: Methyl orange; Adsorption; Activated carbon; Pine sawdust; pseudo-second-order

Contact information: a: Department of Biochemistry, College of Science, King Saud University, P.O. Box 2455, Riyadh 11451, Saudi Arabia; b: Nuclear Research Center, Atomic Energy Authority, P.O. Box 13759, Inshas, Cairo, Egypt; c: Department of Botany and Microbiology, College of Science, King Saud University, P.O. Box 2455, Riyadh 11451, Saudi Arabia; *Corresponding author: syakout@ksu.edu.sa

INTRODUCTION

Wastewater effluents from different kinds of industries have many kinds of synthetic dyes. These industries include leather, textile, plastic, cosmetics, food processing, paper, pharmaceutical, printing, and dye manufacturing. Most of the dyes are stable to light and oxidation and are non-biodegradable (Javaid *et al.* 2011). They are also toxic if they go directly into marine environments. Dyes can be carcinogenic and mutagenic and they can create several serious human health problems. For these reasons, they should be treated before being released into bodies of water (Ajjji and Ali 2007).

Several biological, chemical, and physical methods have been used to remove dyes from wastewater. These methods include photochemical, biological degradation, coagulation, flotation, chemical oxidation, reverse osmosis, and adsorption (Gilbert *et al.* 2011; Agarwal *et al.* 2016a,b, 2017; Bhowmik *et al.* 2016, 2018a,b). Comparatively, because of convenience, ease of operation and simplicity of design, adsorption represents one of the most operative and cost-effective methods. Adsorption processes have been widely used in the water and wastewater related industries (Debnath, *et al.* 2016a,b,c, 2017)

Sorption on activated carbons is usually used in dye removal due to its high capability to remove most of the chemical components (Tan *et al.* 2008; Ghasemi *et al.* 2016; Mashhadi *et al.* 2016). This is due to activated carbon's large surface area, microporous character, and adequate porous and chemical features (Bautista-Toledo *et al.* 1994).

Nevertheless, commercial activated carbon is expensive due to the high cost of the starting raw material. For this reason, various types of research has been conducted relative to activated carbon preparation from low-cost and available raw material including agricultural byproducts, such as maize cob waste, fly ash, and sunflower seed hull (Hameed 2008).

Sawdust is a byproduct of lumber manufacturing that is either used as cooking fuel or packaging material. Wood sawdust does not clearly swell in water and does not break down when contact with water is delayed. It can be used as a low-cost sorbent due to its lignocellulosic structure. It includes cellulose, lignin, hemicellulose, and some functional groups (*e.g.*, carboxyl, phenolic, hydroxyl, *etc.*) in its structure that make sorption achievable. Many studies have been conducted on the use of wood sawdust for the removal of pollutants from aqueous solutions.

The present study aims to investigate the potential use of pine sawdust (PSD) for the preparation of activated carbon and using it for methyl orange (MO) sorption. Phosphoric acid pine sawdust activated carbon (PSDP) will be characterized in this study. The kinetic and equilibrium data will be investigated using different models to recognize the sorption mechanism of MO on PSDP.

The novelty of this study lies in selection of the abundantly available sawdust as precursor and in tailoring the preparation method of biosorbent to remove methyl orange from aqueous solution. The processing and transformation of sawdust into adsorbent with good adsorption properties would alleviate negative impacts of direct burning and disposal of these waste by-products, while producing value added products for water and wastewater treatment.

EXPERIMENTAL

Materials

Preparation of MO solution

A total of 1000 ppm MO stock solution (BDH, London, England) was prepared by dissolving the required amount of the analytical reagent grade MO in the least amount of double distilled water (DDW), and then it was transferred to a volumetric flask and filled up to the mark with double distilled water. Various concentrations (less than or equal 100 ppm) were prepared by stock solution dilution.

Production of activated carbon

Pine (*Pinus strobus*) sawdust was collected from a local Egyptian industrial unit (Selvada furniture, Cairo, Egypt). To eliminate the dirt and impurities from the PSD, it was washed several times with double distilled water (DDW) and dried at 120 °C for 72 h. The PSD was utilized for the production of sorbents through both physical and chemical activation.

In this phase, one stage of thermal-chemical activation with several acids and bases was utilized for the production of activated carbon (Wahi *et al.* 2017). Beginning with 25 g of the squashed PSD, it was imbibed in 55 mL of pre-diluted NaOH or pre-diluted acids including phosphoric acid or oxalic acid to coat it totally. Then the mixture was shaken for some time to confirm entrance of the solution through it and left overnight at room temperature. The impregnated mass was dried out in an oven at 80 °C overnight. It was introduced into a tubular electric furnace with a temperature rate of 50 °C / 20 min up to

600 °C and held for 100 min. After gradual cooling down to room temperature, the activated carbon was continually cleaned with hot DDW until a pH greater than 5 was reached. The cleaned carbon was dried at 120 °C for 24 h and then stored in a desiccator for later use. The prepared activated carbons and their abbreviations are shown in Table 1.

Table 1. Abbreviations of Activated Carbons Prepared from Pine Sawdust

Sample Notation	Preparation Conditions
PSD	Pine sawdust with no treatment
PSDP	Activation using H ₃ PO ₄ at 600 °C for 100 min
PSDNa	Activation using NaOH at 600 °C for 100 min
PSDOX	Activation using oxalic acid at 600 °C for 100 min

Methods

Activated carbon characterization

A nitrogen adsorption analyzer (NOVA 1000e; Quantachrome Corporation, Boynton Beach, FL, USA) at -196 °C was used to measure the Brunauer–Emmett–Teller (BET) surface area of PSDP. The surface functional groups of the PSDP sample were examined utilizing a Fourier transform infrared spectrometer (Shimadzu, Kyoto, Japan) in the range of 500 to 4000 cm⁻¹. The suspension pH (pHSUS) relates carbon acidity or basicity and was measured from a suspension of 0.4 g of PSDP in 40 mL of distilled water that was equilibrated for 72 h at room temperature. Carbon ash (mass difference before and after drying in an oven at 750 °C) and moisture content (mass difference before and after drying in an oven at 150 °C) were measured. Carbon apparent and packed densities were determined by filling a graduated cylinder with specific mass and the volume was measured as (cm³) before and after packing.

Adsorption measurements using the batch method

The sorption study was achieved by batch sorption with MO as an adsorbate and PSDP as an adsorbent. A total of 1000 mg·L⁻¹ of dye stock solution was used to obtain the required working concentrations (100 mg·g⁻¹). Measurements of MO dye and its calibration curve were performed at the wavelength of greatest absorbance (λ_{max} of 463 nm). Then a 0.1 N NaOH or 0.1 N HCl solution was used to adjust the solution pH. A temperature controlled water bath shaker was used in the adsorption experiments. The influences of several different parameters, including pH, contact time, and initial concentration, were examined. Blanks without carbon were used in all of the experiments. The highest removal of MO was achieved at the minimum pH value tested (pH = 1.7) and initial MO solution concentration of 100 mg/L. These conditions were used for the rest of adsorption experiments.

In the adsorption experiment, 0.01 g of PSDP was added to an Erlenmeyer flask that had 10 mL of dye with a 100 mg/L initial concentration, pH=1.7, and temperature of 25 °C. The flask was then shaken until equilibrium was reached. At that time, the carbon was isolated from the solution *via* filtration using Whatman 44 filter paper (Whatman, New York, USA). The dye solution concentration was measured *via* an ultraviolet-visible (UV-Vis) spectrophotometer (160-A; Shimadzu, Kyoto, Japan) using the calibration curve of absorbance against concentration at maximum absorbance $\lambda = 463$ nm.

The amount of MO amount of dye adsorbed in mg·g⁻¹ at time t was measured using the following mass balance Eq. 1,

$$q_t = (C_o - C_e) \times (V/M) \quad (1)$$

where q_t is the equivalent to the equilibrium at a contact time (mg/g), C_e is the concentration at equilibrium (mg/L), C_o is the initial concentration (mg/L), V is the solution volume (mL), and M is the adsorbent mass (g).

The sorption efficiency (%) was calculated using Eq. 2,

$$\text{Sorption (\%)} = ((C_o - C_e)/C_o) \times 100 \quad (2)$$

RESULTS AND DISCUSSION

Adsorbents Characterization

Several of the physicochemical characterizations of different carbons are given in Table 2, which indicates the variation in their properties consistent with the preparation method. Table 3 provides the BET surface area (S_{BET}), total pore volume (V_{total}), and average pore radius that calculated from nitrogen adsorption isotherm in Fig. 1 of the PSDP carbon prepared at the optimum conditions.

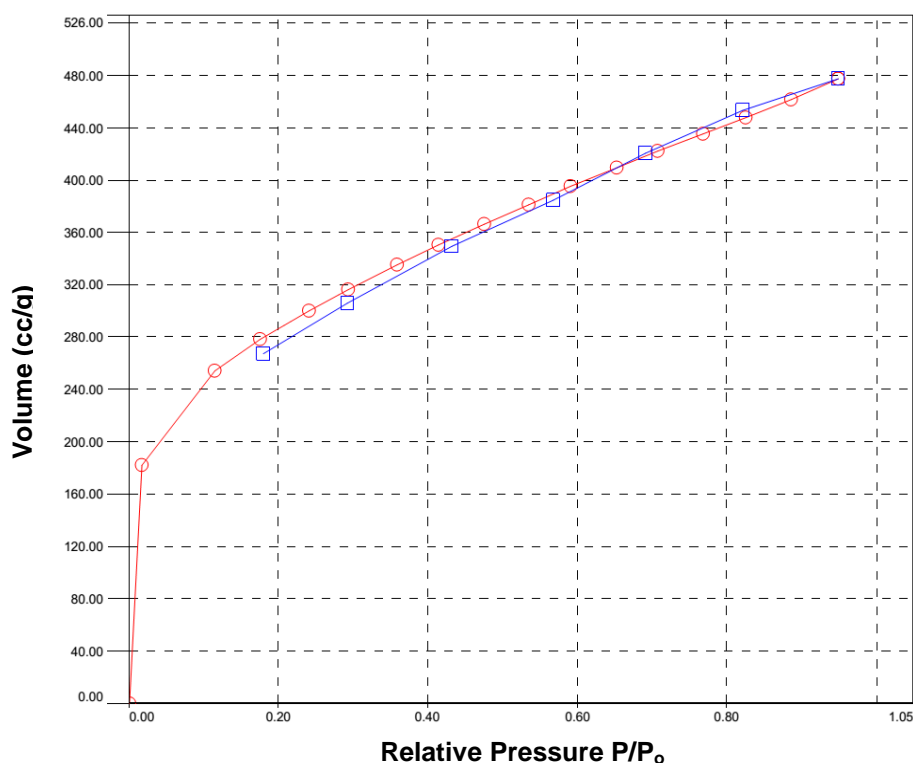


Fig. 1. Isotherm linear adsorption of nitrogen by PSDP sample

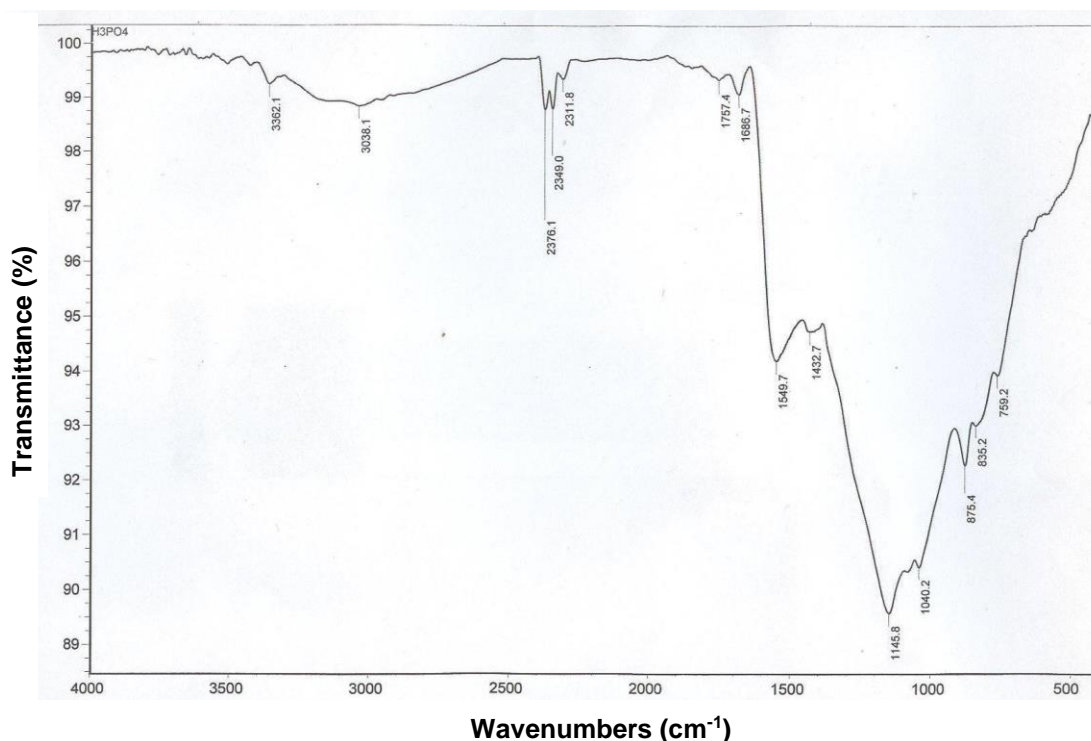
Table 2. Physicochemical Characterizations of Prepared Sorbents

Samples	Yield (%)	pHSUS	Moisture (%)	Density (g/cm ³)		Ash (%)
				Apparent	Packed	
PSD	100	5.2	10.7	0.16	0.31	1.6
PSDP	64.57	6.5	6.87	0.32	0.41	22
PSDNa	65.27	8.5	4.08	0.13	0.18	18.59
PSDOX	17.33	7.5	3.95	0.32	0.43	10.3

Table 3. Surface Characterization of Prepared PSDP Samples

Methods	Parameter	Values
BET	Surface area (m ² /g)	991.14
	Total pore volume (cm ³ /g)	7.385e ⁻⁰¹
	Average pore radius (nm)	1.49 e ⁺⁰¹
Langmuir	Surface area (m ² /g)	1449.64

For FTIR spectra of PSDP carbon in Fig. 2, bands at around 3401 and 1080 cm⁻¹ are assigned to the –OH vibrations and hence indicating the presence of surface hydroxyl groups. The band at 3401 cm⁻¹ may be due to both free and hydrogen bonded O–H groups. The triplet in bands in the region 1200 to 1000 cm⁻¹ was considered to result from the superposition of vibrations of the C–OH bond. The absorption bands at the 2377 to 2310 cm⁻¹ region commonly appear from triple bonds and other restricted types of functional groups. The band around 1685.7 cm⁻¹ is usually caused by the stretching vibration of C=O in aldehydes, ketones, carboxyl groups and lactones; this peak maybe bears slight overlapping with C=C aromatic ring stretching vibration which is commonly located at 1556.6 cm⁻¹.

**Fig. 2.** FTIR spectra of PSDP carbon

An SEM micrograph for PSDP with magnification at 2000x is shown in Fig. 3. The PSDP prepared at 500 °C has well-developed pore structure, indicative of a high surface area and therefore supporting the surface area and porosity. It seems that the cavities on the surfaces of carbons resulted from the evaporation of the activating agent, which in this case is phosphoric during carbonization, leaving the space previously occupied by the activating agent.

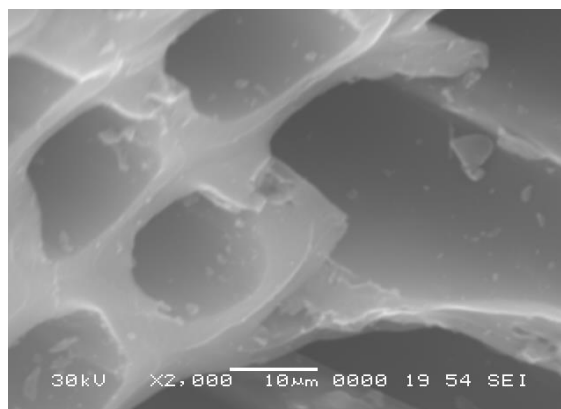


Fig. 3 SEM of PSDP carbon

Preliminary Adsorption Investigation

The main task was to investigate each suitably prepared carbon and select which one should be used for the removal of MO from aqueous solution. According to the results in Table 4, there was a noticeable variance in the adsorption capacity of the four adsorbents used to remove MO from aqueous solution. This indicated that different adsorption mechanisms controlled the interactions between these carbon surfaces and MO in the aqueous solution.

Table 4. A Preliminary Test for Selection of Adsorbent Samples

No.	Sample Notation	MO Uptake (mg/g)
1	PSD	2.1
2	PSDP	84.7
3	PSDNa	21.8
4	PSDOX	39.5

The PSDP was found superior in the removal of MO. Therefore, PSDP was selected for further investigation. The optimization of the adsorption of MO in aqueous solution by modified sawdust based carbon was achieved through altering various parameters (*e.g.*, initial concentration, equilibrium time, and pH) and will be discussed in the following section. The criterion used for the optimization was the selection of parameters where maximum adsorption occurred.

Effect of pH on the Adsorption of MO onto PSDP

Solution pH has an essential role in the entire sorption procedure, affecting not only MO solution chemistry but also carbon surface charge and dissociation of its functional groups at active sites. The influence of the initial MO solution pH on its adsorption onto PSDP is shown in Fig. 4. The MO adsorption onto the PSDP strongly depended upon the pH. In general, MO adsorption in an acidic medium is greater than in an alkaline medium. Similar results of the influence of pH for the adsorption of MO onto activated carbon have been reported (Ghaedi *et al.* 2014). The highest removal of MO was achieved at the minimum pH value tested (pH = 1.7) under the present experimental conditions (initial MO solution concentration of 100 mg/L). A decrease in the solution pH from 9 to 1.7 caused a remarkable increase in MO adsorption from 28 to 99 mg/g for PSDP.

A possible explanation of pH effect on MO adsorption is the change of adsorbent surface charge and MO ionization degree. At very high acidic medium, PSDP surface

become highly protonated, acquiring positive charge and MO ionization degree reach its maximum ($pK_a = 3.46$, Subbaiah and Kim 2016). These conditions motivated the electrostatic attraction between the MO and the positive active site (Zayed *et al.* 2018). Also, PSDP has hydroxyl groups on its surface. In acid solutions the hydroxyl groups of carbon are much easier to be cationized. The adsorption of MO on PSDP could be due to a replacement of MO for OH group on carbon surface. (Haldorai and Shim 2014).

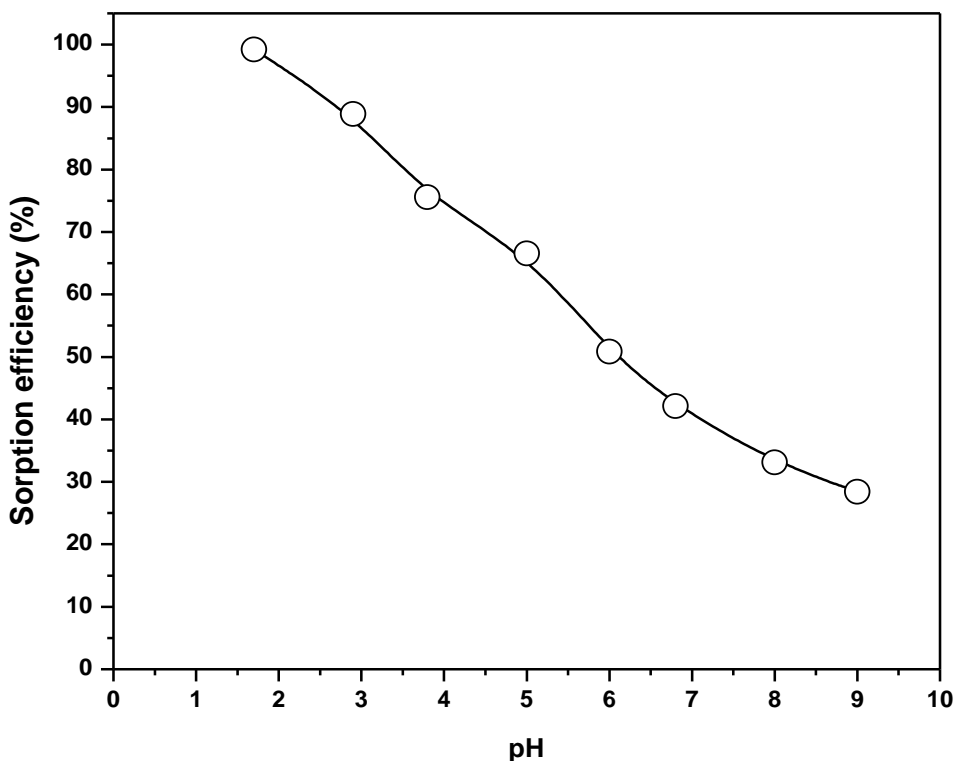
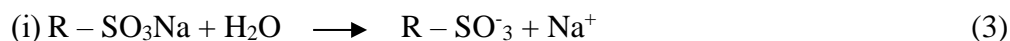


Fig. 4. Effect of pH on adsorption of MO by PSDP; conditions: $V = 10$ mL; $m = 0.01$ g; and $C_0 = 100$ mg/L

Sorption Mechanism of Methyl Orange

The MO sorption mechanism onto PSDP takes place through two main stages. The 1st stage happens when the pH value decreases; the PSDP surface consumes more H^+ ions from the solution and thus becomes more acidic and positive. At that time, when MO is dissolved in this aqueous acidic solution, the sulfonate groups ($R-SO_3Na$) on the MO molecules are dissociated and changed into anionic dye ions ($R-SO_3^-$) as seen in Eq. 3:



Therefore, in the 2nd stage adsorption was achieved due to electrostatic attractions between the MO's anionic molecules and carbon surfaces ($\acute{S}-OH^+$), or due to a replacement of anionic dye ions ($R-SO_3^-$) for OH group on carbon surface as clear from Eq. 4:



Nevertheless, increasing the value of the MO solution pH decreased the adsorption. This decrease can be explained by the competition of OH^- ions and MO anions for adsorption sites in a basic solution (Huang *et al.* 2017).

Influence of Agitation Time

The effect of agitation time on the adsorption of MO using PSDP is given in Fig. 5. As agitation time increased, the MO removal rapidly increased and then slowed down until reaching steady constant adsorption after 72 h, which indicated the achievement of equilibrium and after which there was no further increment in the adsorption. The curve in Fig. 5 showed the initial fast removal of MO followed by a noticeable decrease in the rate as the rate of change approached zero, *i.e.*, equilibrium was attained. Alterations in the removal rate could have been due to the fact that at the start, adsorption sites were empty and the MO concentration gradient was high. Afterward, the removal rate of MO molecules by PSDP decreased noticeably as a result of the reduction of vacant adsorption sites on the carbon surfaces. Specifically, at low surface coverage, adsorbed MO molecules initially filled the highest energy sites, and once these became saturated the MO molecules gradually occupied the lower energy sites, which resulted in the decrease of the average binding energy on the surface.

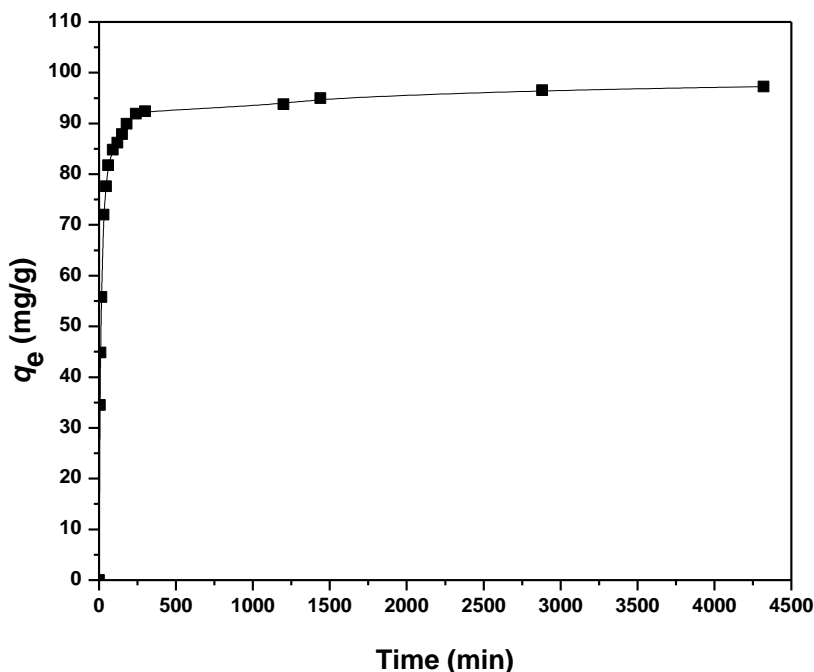


Fig. 5. Effect of agitation time on adsorption of MO on PSDP; conditions: $V = 10$ mL; $\text{pH} = 1.7$; $m = 0.01$ g; and $C_0 = 100$ mg/L

Sorption processes of such types of adsorbate include three-steps (Moussavi and Khosravi 2010): (i) exterior film diffusion through the surrounding particle boundary layer, (ii) intraparticle mass transition inside the adsorbent particle's boundary *via* pore diffusion or homogeneous surface diffusion, and (iii) sorption of the adsorbate molecule at a surface site. External film diffusion is frequently important in the rate-controlling process. However, intraparticle diffusion frequently has a much greater effect on equilibrium time and saturation capacity.

PSDP carbon was found to be superior for MO removal. The value of the adsorption capacity q (91.9 mg/g) was high in comparison to several other reported low-cost adsorbents such as 77.0 mg/g for commercially-activated carbon (Martini *et al.* 2018), 50.8 mg/g for chitosan/rectorite/carbon nanotubes composite (Chen *et al.* 2017), and 67.9 for

fly ash modified by $\text{Ca}(\text{OH})_2/\text{Na}_2\text{FeO}_4$ (Gao *et al.* 2015), Therefore the utilization of such unused resources from an agricultural waste as an alternative adsorbent for MO removal is highly desirable.

Adsorption Kinetics

Two kinetic models were examined and used to fit the experimental adsorption data of MO onto PSDP.

Pseudo-first-order kinetic adsorption model

This model can be expressed by the Lagergren rate equation,

$$\log(q_e - q_t) = \log(q_e) - \frac{k_1}{2.303} t \quad (5)$$

where q_e and q_t are the amounts of MO (mg/g) at equilibrium and time t , respectively, K_1 is the pseudo-first-order constant (min^{-1}). q_e can be calculated from the slope and intercept of the plot of $\log(q_e - q)$ versus time (Fig. 6a and Table 5). It was clear that MO adsorption onto PSDP did not follow the pseudo-first-order model due to the low correlation coefficient ($R^2 = 0.861$) and the great difference between the calculated q_e values ($q_{e, \text{cal}} = 38.45$ mg/g) and experimental data ($q_{e, \text{exp}} = 91.89$ mg/g).

Pseudo-second-order kinetic model

This model can be expressed by the following Eq. 6,

$$\frac{t}{q_t} = \frac{1}{k_2 q_e^2} + \frac{1}{q_e} t \quad (6)$$

where q_t is the amount adsorbed (mg/g) at time t and K_2 is the second-order rate constant (g/mg. min) that can be calculated from the plot of (t / q_t) versus t (Fig. 6b and Table 5).

According to the coefficient of determination ($R^2 = 0.999$), $q_{e, \text{exp}}$ (91.89 mg/g), and $q_{e, \text{cal}}$ (94.87mg/g) in Table 5, the pseudo-second-order kinetic model can be used to represent MO adsorption onto PSDP. The second-order equation is also based on the sorption capacity of the solid phase. Contrary to the other model, it predicts the behavior over the whole range of adsorption.

Table 5. Pseudo-first-order and Pseudo-second-order Adsorption Rate Constants for MO

Model	Parameter	Methyl Orange
Pseudo-first-order model	$q_{e, \text{exp}}$ (mg/g)	91.89
	K_1 (min^{-1})	0.014
	$q_{e, \text{cal}}$ (mg/g)	38.45
	R^2	0.861
Second-order model	K_2 (g/mg min)	9.8×10^{-4}
	h (mg/g min)	8.84
	$q_{e, \text{cal}}$ (mg/g)	94.87
	R^2	0.999
Intraparticle parameter	K_{id} (mg/g $\text{min}^{0.5}$)	1.08
	R^2	0.979

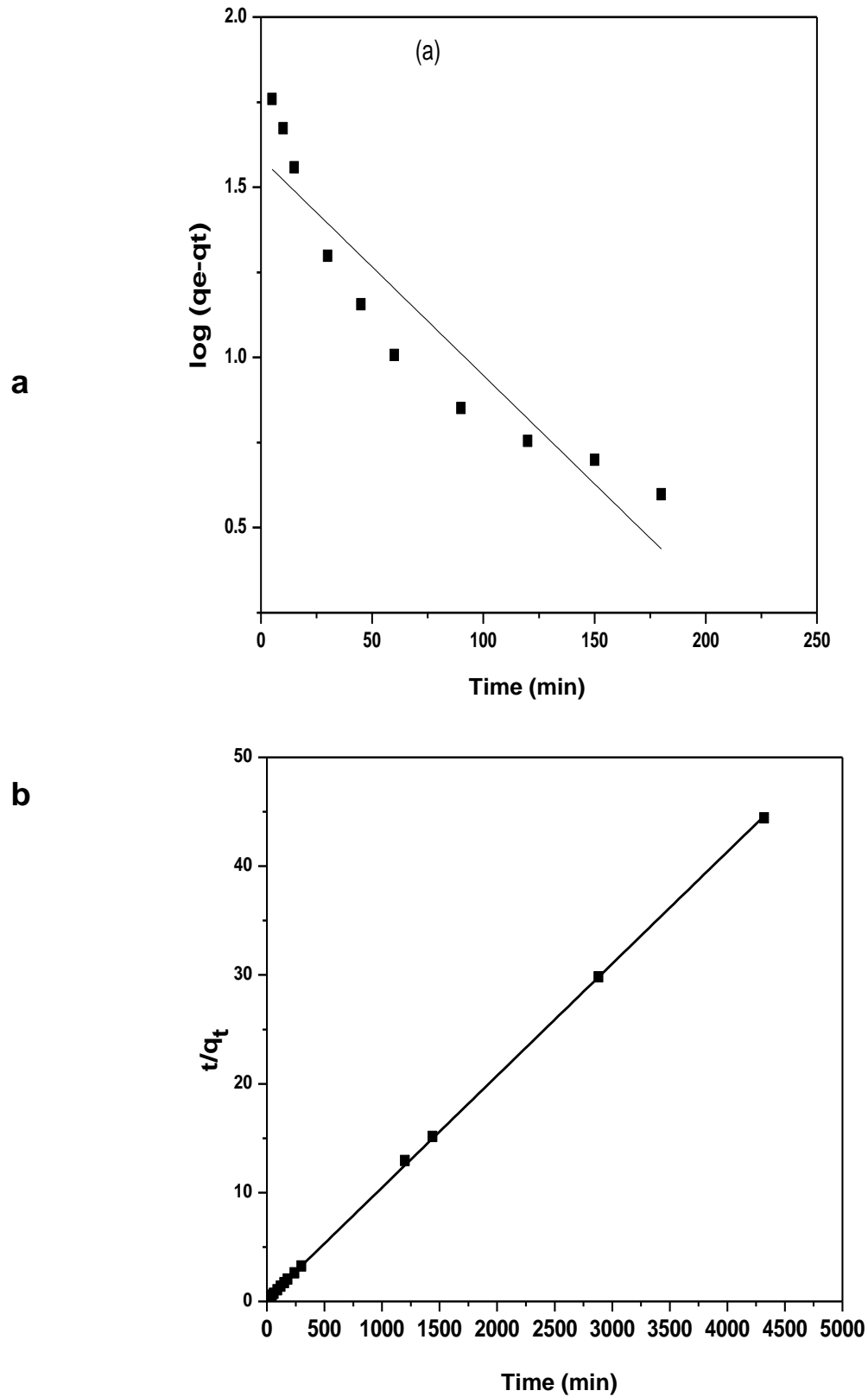


Fig. 6. (a) Pseudo-first-order sorption kinetics of MO on PSDP and (b) pseudo-second-order sorption kinetics of MO on PSDP

Intraparticle Diffusion

The above kinetic models were not able to distinguish between the different diffusion mechanisms. In the intraparticle diffusion model developed by Weber and Morris (1963), the rate of intraparticle diffusion is a function of $t^{0.5}$ (Gad *et al.* 2016). According to this theory, the intraparticle diffusion equation is expressed as follows,

$$q_t = K_{id}t^{0.5} + C \quad (7)$$

where C (mg/L) is the intercept and K_{id} is the slope (intraparticle diffusion rate constant, $[\text{mg/g}] \cdot \text{min}^{0.5}$) of the plot of q_t versus $t^{1/2}$ (Fig. 7).

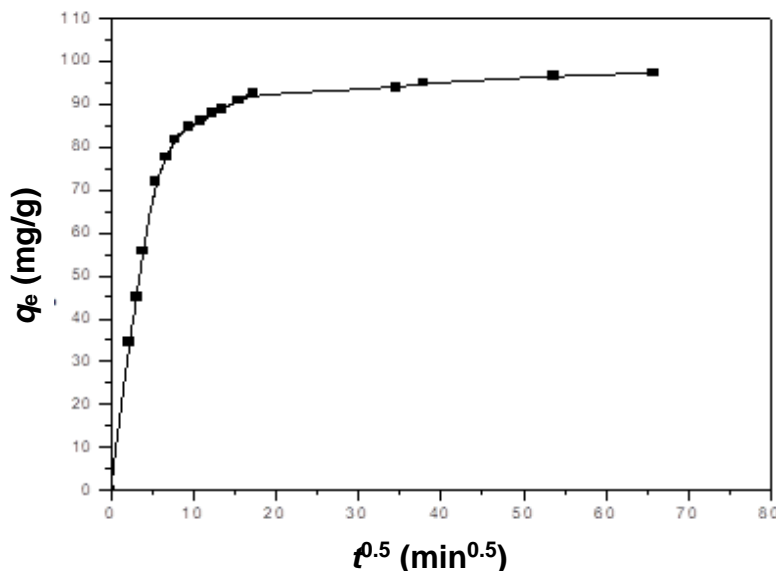


Fig. 7. Intraparticle diffusion plots for MO adsorption onto PSDP

The plot of the present study did not make a straight line throughout the whole time, which indicated that that the intraparticle diffusion was not the only rate-controlling step. The adsorption mechanism of MO adsorption by PSDP is a rather complex process, most likely a combination of external mass transfer and intraparticle diffusion that contribute to the rate-determining step (Khaled *et al.* 2009).

Effect of Adsorbent Mass on the Adsorption of Methyl Orange

The adsorbent mass is a vital parameter in adsorption examinations because it decides the capacity of the adsorbent for a given initial concentration of adsorbate solution. The impact of adsorbent mass on the adsorption capacity and percent adsorption is shown in Fig. 8.

An increased adsorbent mass led to a rapid increase in adsorption percentage (R%) and decreased adsorption capacity (q_e). An increase in the adsorbent mass from 5 to 15 mg increased the percentage of MO removal by PSDP from 65% to 100%. This was because increasing the adsorbent mass leads to an increase in available sorption sites (Zakaria *et al.* 2009).

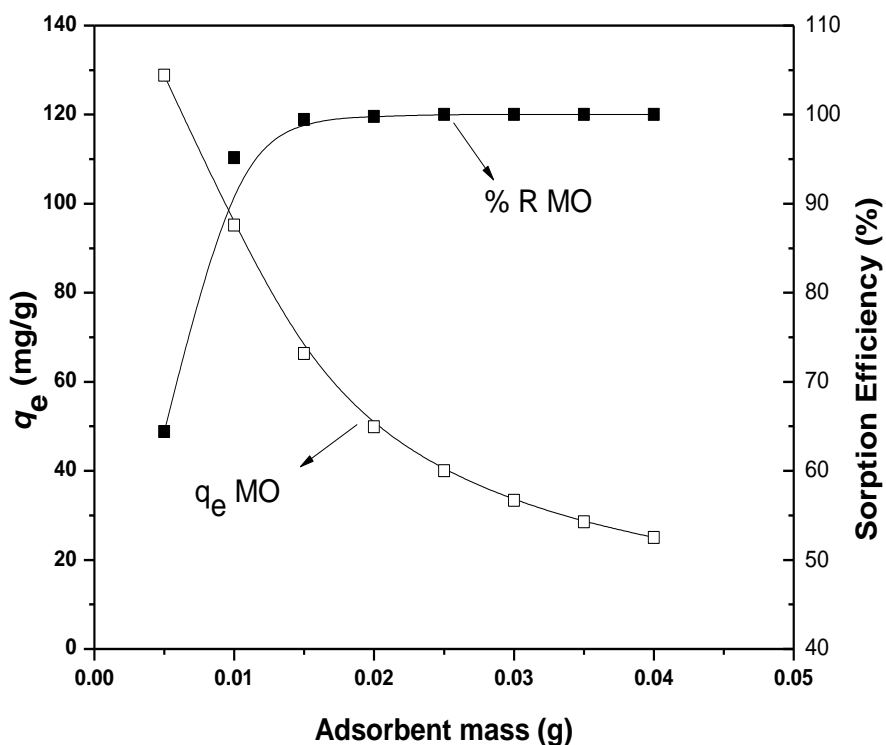


Fig. 8. Effect of adsorbent mass uptake and percent removal of MO; conditions: $V = 10$ mL; $\text{pH} = 1.7$; $m = 0.005 - 0.04$ g; $C_0 = 100$ mg/L; and $T = 25$ °C

CONCLUSIONS

1. The present study concluded that pine sawdust (PSD) can be utilized for the preparation of a new adsorbent through various treatment strategies prompting distinctive characteristics and practices.
2. Fourier transform infrared spectroscopy demonstrated that pine sawdust activated carbon (PSDP) contained numerous functional groups. These functional groups may take part in methyl orange (MO) adsorption.
3. Experimental results showed that maximum MO adsorption by PSDP took place at a pH of 1.7.
4. Kinetic data indicated that the adsorption followed the pseudo-second-order model.
5. Therefore, the current investigation showed that the PSDP has encouraging usages for the removal of MO molecules from aqueous solution.

ACKNOWLEDGMENTS

The authors extend their appreciation to the Deanship of Scientific Research at King Saud University for funding this work through research group no (RG-1440-043).

REFERENCES CITED

- Agarwal, S., Tyagi, I., Gupta, V. K., Ghasemi, N., Shahivand, M., and Ghasemi, M. (2016). "Kinetics, equilibrium studies and thermodynamics of methylene blue adsorption on *Ephedra strobilacea* saw dust and modified using phosphoric acid and zinc chloride," *Journal of Molecular Liquids* 218, 208-218. DOI: 10.1016/j.molliq.2016.02.073
- Agarwal, S., Tyagi, I., Gupta, V. K., Mashhadi, S., and Ghasemi, M. (2016). "Kinetics and thermodynamics of Malachite Green dye removal from aqueous phase using iron nanoparticles loaded on ash," *Journal of Molecular Liquids* 223, 1340-1347. DOI: 10.1016/j.molliq.2016.04.039
- Agarwal, S., Gupta, V. K., Ghasemi, M., and Azimi-Amin, J. (2017). "*Peganum harmala*-L Seeds adsorbent for the rapid removal of noxious brilliant green dyes from aqueous phase," *Journal of Molecular Liquids* 231, 296-305. DOI: 10.1016/j.molliq.2017.01.097
- Ajji, Z., and Ali, A. M. (2007). "Adsorption of methyl violet and brilliant blue onto poly (vinyl alcohol) membranes grafted with N-vinyl imidazole/acrylic acid," *Nuclear Instruments and Methods in Physics Research Section B: Beam Interactions with Materials and Atoms* 265(1), 362-365. DOI: 10.1016/j.nimb.2007.09.004
- Bautista-Toledo, I., Rivera-Utrilla, J., Ferrero-García, M. A., and Moreno-Castilla, C. (1994). "Influence of the oxygen surface complexes of activated carbons on the adsorption of chromium ions from aqueous solutions: Effect of sodium chloride and humic acid," *Carbon* 32(1), 93-100. DOI: 10.1016/0008-6223(94)90013-2
- Bhowmik, K. L., Debnath, A., Nath, R. K., Das, S., Chattopadhyay, K. K., and Saha, B. (2016). "Synthesis and characterization of mixed phase manganese ferrite and hausmannite magnetic nanoparticle as potential adsorbent for methyl orange from aqueous media: Artificial neural network modeling," *Journal of Molecular Liquids* 219, 1010-1022. DOI: 10.1016/j.molliq.2016.04.009
- Bhowmik, K. L., Debnath, A., Nath, R. K., and Saha, B. (2017). "Synthesis of $MnFe_2O_4$ and Mn_3O_4 magnetic nano-composites with enhanced properties for adsorption of Cr(VI): Artificial neural network modeling," *Water Science and Technology* 76(12), 3368-3378. DOI: 10.2166/wst.2017.501
- Bhowmik, M., Deb, K., Debnath, A., and Saha, B. (2018a). "Mixed phase Fe_2O_3/Mn_3O_4 magnetic nanocomposite for enhanced adsorption of methyl orange dye: Neural network modeling and response surface methodology optimization," *Applied Organometallic Chemistry* 32(3), e4186. DOI: 10.1002/aoc.4186
- Bhowmik, M., Debnath, A., and Saha, B. (2018b). "Fabrication of mixed phase calcium ferrite and zirconia nanocomposite for abatement of methyl orange dye from aqua matrix: Optimization of process parameters," *Applied Organometallic Chemistry* 32(12), e4607. doi: 10.1002/aoc.4607
- Chen, J., Shi, X., Zhan, Y., Qiu, X., Du, Y., and Deng, H. (2017). "Construction of horizontal stratum landform-like composite foams and their methyl orange adsorption capacity," *Applied Surface Science* 397, 133-143. DOI: 10.1016/j.apsusc.2016.10.211
- Debnath, A., Deb, K., Chattopadhyay, K. K., and Saha, B. (2016a). "Methyl orange adsorption onto simple chemical route synthesized crystalline α - Fe_2O_3 nanoparticles: Kinetic, equilibrium isotherm, and neural network modeling,"

- Desalination and Water Treatment* 57(29), 13549-13560. DOI: 10.1080/19443994.2015.1060540
- Debnath, A., Deb, K., Das, N. S., Chattopadhyay, K. K., and Saha, B. (2016b). "Simple chemical route synthesis of Fe₂O₃ nanoparticles and its application for adsorptive removal of congo red from aqueous media: artificial neural network modeling," *Journal of Dispersion Science and Technology* 37(6), 775-785. DOI: 10.1080/01932691.2015.1062772
- Debnath, A., Majumder, M., Pal, M., Das, N. S., Chattopadhyay, K. K., and Saha, B. (2016c). "Enhanced adsorption of hexavalent chromium onto magnetic calcium ferrite nanoparticles: Kinetic, isotherm, and neural network modeling," *Journal of Dispersion Science and Technology* 37(12), 1806-1818. DOI: 10.1080/01932691.2016.1141100
- Gad, H. M. H., Omar, H. A., Aziz, M., Hassan, M. R., and Khalil, M. H. (2016). "Treatment of rice husk ash to improve adsorption capacity of cobalt from aqueous solution," *Asian Journal of Chemistry* 28(2), 385-394. DOI: 10.14233/ajchem.2016.19364
- Gao, M., Ma, Q., Lin, Q., Chang, J., Bao, W., and Ma, H. (2015). "Combined modification of fly ash with Ca(OH)₂/Na₂FeO₄ and its adsorption of methyl orange," *Applied Surface Science* 359, 323-330. DOI: 10.1016/j.apsusc.2015.10.135
- Ghaedi, M., Ghaedi, A. M., Ansari, A., Mohammadi, F., and Vafaei, A. (2014). "Artificial neural network and particle swarm optimization for removal of methyl orange by gold nanoparticles loaded on activated carbon and Tamarisk," *Spectrochimica Acta Part A: Molecular and Biomolecular Spectroscopy* 132, 639-654. DOI: 10.1016/j.saa.2014.04.175
- Ghasemi, M., Mashhadi, S., Asif, M., Tyagi, I., Agarwal, S., and Gupta, V. K. (2016). "Microwave-assisted synthesis of tetraethylenepentamine functionalized activated carbon with high adsorption capacity for malachite green dye," *Journal of Molecular Liquids* 213, 317-325. DOI: 10.1016/j.molliq.2015.09.048
- Gilbert, U. A., Emmanuel, I. U., Adebajo, A. A., and Olalere, G. A. (2011). "Biosorptive removal of Pb²⁺ and Cd²⁺ onto novel biosorbent: Defatted *Carica papaya* seeds," *Biomass and Bioenergy* 35(7), 2517-2525. DOI: 10.1016/j.biombioe.2011.02.024
- Haldorai, Y., and Shim, J. (2014). "An efficient removal of methyl orange dye from aqueous solution by adsorption onto chitosan/MgO composite: A novel reusable adsorbent," *Applied Surface Science* 292, 447-453. DOI: 10.1016/j.apsusc.2013.11.158
- Hameed, B. H. (2008). "Equilibrium and kinetic studies of methyl violet sorption by agricultural waste," *Journal of Hazardous Materials* 154(1), 204-212. DOI: 10.1016/j.jhazmat.2007.10.010
- Huang, R., Liu, Q., Huo, J., and Yang, B. (2017). "Adsorption of methyl orange onto protonated cross-linked chitosan," *Arabian Journal of Chemistry* 10(1), 24-32. DOI: 10.1016/j.arabjc.2013.05.017
- Javaid, A., Bajwa, R., Shafique, U., and Anwar, J. (2011). "Removal of heavy metals by adsorption on *Pleurotus ostreatus*," *Biomass and Bioenergy* 35(5), 1675-1682. DOI: 10.1016/j.biombioe.2010.12.035
- Khaled, A., Nemr, A. E., El-Sikaily, A., and Abdelwahab, O. (2009). "Treatment of artificial textile dye effluent containing Direct Yellow 12 by orange peel carbon," *Desalination* 238(1-3), 210-232. DOI: 10.1016/j.desal.2008.02.014

- Martini, B. K., Daniel, T. G., Corazza, M. Z., and de Carvalho, A. E. (2018). "Methyl orange and tartrazine yellow adsorption on activated carbon prepared from boiler residue: Kinetics, isotherms, thermodynamics studies and material characterization," *Journal of Environmental Chemical Engineering* 6(5), 6669-6679. DOI: 10.1016/j.jece.2018.10.013
- Mashhadi, S., Javadian, H., Ghasemi, M., Saleh, T. A., and Gupta, V. K. (2016). "Microwave-induced H₂SO₄ activation of activated carbon derived from rice agricultural wastes for sorption of methylene blue from aqueous solution," *Desalination and Water Treatment* 57 (44), 21091-21104. DOI:10.1080/19443994.2015.1119737
- Moussavi, G., and Khosravi, R. (2010). "Removal of cyanide from wastewater by adsorption onto pistachio hull wastes: Parametric experiments, kinetics and equilibrium analysis," *Journal of Hazardous Materials* 183(1), 724-730. DOI: 10.1016/j.jhazmat.2010.07.086
- Subbaiah, M. V., and Kim, D.-S. (2016). "Adsorption of methyl orange from aqueous solution by aminated pumpkin seed powder: Kinetics, isotherms, and thermodynamic studies," *Ecotoxicology and Environmental Safety* 128, 109-117. DOI: 10.1016/j.ecoenv.2016.02.016
- Tan, I. A. W., Ahmad, A. L., and Hameed, B. H. (2008). "Preparation of activated carbon from coconut husk: Optimization study on removal of 2,4,6-trichlorophenol using response surface methodology," *Journal of Hazardous Materials* 153(1), 709-717. DOI: 10.1016/j.jhazmat.2007.09.014
- Wahi, R., Zuhaidi, N. F. Q., Yusof, Y., Jamel, J., Kanakaraju, D., and Ngaini, Z. (2017). "Chemically treated microwave-derived biochar: An overview," *Biomass and Bioenergy* 107, 411-421. DOI: 10.1016/j.biombioe.2017.08.007
- Zakaria, Z. A., Suratman, M., Mohammed, N., and Ahmad, W. A. (2009). "Chromium(VI) removal from aqueous solution by untreated rubber wood sawdust," *Desalination* 244(1-3), 109-121. DOI: 10.1016/j.desal.2008.05.018
- Zayed, A. M., Abdel Wahed, M. S. M., Mohamed, E. A., and Sillanpää, M. (2018). "Insights on the role of organic matters of some Egyptian clays in methyl orange adsorption: Isotherm and kinetic studie," *Applied Clay Science* 166, 49-60. DOI: 10.1016/j.clay.2018.09.013

Article submitted: January 5, 2019; Peer review completed: March 17, 2019; Revised version received: April 1, 2019; Accepted: April 9, 2019; Published: April 23, 2019. DOI: 10.15376/biores.14.2.4560-4574